CrystEngComm

Accepted Manuscript

ROYAL SOCIETY OF CHEMISTRY

www.rsc.org/crystengcomm

CrystEngComm

ARTICLE

A serials of Zn(II) and Cd(II) coordination compounds based on 4-(4*H*-1,2,4-triazol-4-yl)benzoic acid : synthesis, structure and photoluminescent properties

Li-Bo Yang, Hong-Can Wang, Xiao-Dan Fang , Si-Jin Chen, Quan-Qing Xu, Ai-Xin Zhu* and Zhi Yang*

Seven coordination compounds, namely, $[Zn(4\text{-tba})_2(H_2O)_2]$ (**1**), $[Zn(4\text{-tba})Cl]\cdot CH_3OH$ (**2**), $[Zn(4\text{-tba})_2]$ (**3**), $[Zn(4\text{-tba})_2]\cdot DMA\cdot 3.5H_2O$ (**4**), $[Cd(4\text{-tba})_2]\cdot DMF\cdot 3.6H_2O$ (**5**), $[Cd(4\text{-tba})_2]$ (**6**), and $[Cd_5Cl_4(4\text{-tba})_6]\cdot 1.5DMF\cdot 4H_2O$ (**7**) (4-Htba = 4-(4*H*-1,2,4-triazol-4-yl)benzoic acid, DMA = *N*,*N*-dimethylacetamide and DMF = *N*,*N*-dimethylformamide) have been synthesized under hydro/solvothermal conditions by using a triazolate-carboxylate bifunctional organic ligad 4-Htba. Complexes **1** and **2** exhibit a mononuclear motif and a two-dimensional (2D) network with sql topology, respectively, whereas **3**-**6** display different, interpenetrating structures. Compound **3** shows a 2-fold interpenetrating 2D net with sql topology, **4** and **5** display uninodal 4-connected 4-fold interpenetrating 3D nets with dia (6^6) topology belonging to class Ia and class IIIa, respectively, and compound **6** exhibits a 5-fold interpenetrating dia net (6^6). Complex **7** exhibit a non-interpenetrating 3D framework behaving decanuclear cadmium-chloride chain units and various coordination modes of 4-tba ligands. All the complexes were characterized using sing-crystal X-ray diffraction analyses, powder X-ray diffraction (PXRD), IR spectra and elemental analyses. In addition, the thermogravimetric analysis and solid-state photoluminescence results for **1**-**7** were also investigated.

1. Introduction

The rational design and construction of coordination compounds have received considerable attention over the past ten years because of their intriguing molecular topologies[1] and wide range of potential applications such as gas or liquid adsorption,[2] separation,[3] ion change,[4] catalytic activity,[5] magnetism[6] and sensing.[7] Generally, the construction of coordination compounds is dependent on a variety of factors such as organic ligands,[8] solvent,[9] metal ion,[10] ratio of reactants,[11] and counterion.[12] Of all these, appropriate organic ligands are one of the most important factors because their length, steric effects, and flexibility will lead to diverse structures of coordination compounds. Aromatic polycarboxylate, polypyridine and deprotonated polyazaheterocycles are the most extensively exploited ligands to construct metal complexes.[13] More recently, the azolate-carboxylate bifunctional ligands have attracted considerable attention as another type of useful ligands for the construction

of functional metal coordination polymers.[14-16] Among them, the triazolate-carboxylate bifunctional organic ligand have received special attention, owing to their multi-connectivity abilities, interesting luminescent, magnetic and gas-adsorption properties.[15,16]

The bifunctional ligand 4-(4*H*-1,2,4-triazol-1-yl)benzoic acid (4-Htba, Scheme 1) with two nitrogen and two oxygen potential coordination sites has multiple coordination modes, and also can construct diverse coordination polymers with various secondary building unit (SBU).[16] For example, Murugesu and coworkers utilized 4-Htba as the organic bridging ligands, and synthesized a MIL88 structure with trinuclear cobalt core as a triangular SBU and a cubic coordination polymers with an octanuclear Co(II) cubane core as SBU.[16b,c] Cheng et al. reported a series of 4-tba based Cu(II) MOFs containing various SBUs such as mononuclear, binuclear, trinuclear, tetranuclear and chloride-centered square-planar $[Cu_4Cl]^{7+}$ units.[16d,e] However, the most reported coordination polymers base on this ligand are usually restricted to magnetic metal ions, and their properties are mainly confined to the fields of magnetism and gas or liquid adsorption. The investigation of the 4-tba ligand as building blocks for constructing d^{10} luminescent coordination polymers has been less developed so far.[16a]

Faculty of Chemistry and Chemical Engineering, Yunnan Normal University, Kunming 650500, China. Tel: +86 0871 65941088; Email:zaxchem@126.com and kmyangz@hotmail.com
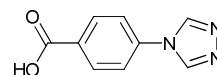
Scheme 1 Structure of 4-(4*H*-1,2,4-triazol-1-yl)benzoic acid (4-Htba)

ARTICLE   **Journal Name**

Herein, a serials of new Zn(II) and Cd(II) coordination compounds based on 4-tba ligand, namely, [Zn(4-tba)$_2$(H$_2$O)$_2$] (**1**), [Zn(4-tba)Cl]·CH$_3$OH (**2**), [Zn(4-tba)$_2$] (**3**), [Zn(4-tba)$_2$]·DMA·3.5H$_2$O (**4**), [Cd(4-tba)$_2$]·DMF·3.6H$_2$O (**5**), [Cd(4-tba)$_2$] (**6**), and [Cd$_5$Cl$_4$(4-tba)$_6$]·1.5DMF·4H$_2$O (**7**), were synthesized under hydro/solvothermal conditions and characterized via X-ray single crystal diffraction. Moreover, the thermogravimetric analysis and solid-state photoluminescence results for **1**-**7** were also studied.

2. Experimental

2.1. Materials and methods

The ligand 4-Htba was synthesized according to the literature method.[15b] Other reagents and solvents were commercially available and were used without further purification. IR spectra were obtained from KBr pellets on a Bruker EQUINOX 55 FT IR spectrometer in the 400-4000 cm^{-1} region. Elemental analyses (C, H, N) were performed with a Vario EL elemental analyzer. The phase-purity and crystallinity of each product were checked by powder X-ray diffraction (PXRD) using a Rigaku D/M-2200T automated diffractometer CuKα, 1.5418 Å). The observed and simulated powder XRD patterns of all compounds are displayed in Fig. S1-S7 in the ESI†. Thermogravimetric analysis (TGA) was performed using a Netzsch STA 449C instrument. Each sample was heated from room temperature to 700 °C with a heating rate of 10.0 °C/min under nitrogen atmosphere. Room-temperature photoluminescence (PL) spectra were recorded using a Hitachi F-4600 fluorescence spectrophotometer equipped with a xenon lamp. For zinc complexes **1-4**, the slit widths of excitation and emission were fixed at 2.5 and 1.0 nm, respectively. For cadmium complexes **5-7**, the slit widths of excitation and emission were fixed at 5.0 and 2.5 nm, respectively.

2.2. Preparation of complexes 1–7

2.2.1. Synthesis of [Zn(4-tba)$_2$(H$_2$O)$_2$] (1). A mixture of ZnCl$_2$ (14 mg, 0.1 mmol), 4-Htba (19 mg, 0.1 mmol), H$_2$O (4 mL), and MeOH (1 mL) was placed in a Teflon-lined stainless steel vessel (15 mL) and heated at 120 °C for 3 days and then cooled to room temperature at a rate of 5°C/h. Colorless, needle-like crystals were collected by filtration, washed with water and dried in air to afford 13 mg (55% based on 4-Hbta) of product. Anal. Calcd. for C$_{18}$H$_{16}$N$_6$O$_6$Zn: C, 45.25; H, 3.38; N, 17.59. Found: C, 45.23; H, 3.39; N, 17.62. IR (cm^{-1}, KBr): 3317(br, m), 1719(m), 1606(s), 1536(s), 1469 (w), 1423(s), 1306(w), 1248(m), 1093(m), 1007(m), 861 (m), 784(m), 696(w), 523(m).

2.2.2. Synthesis of [Zn(4-tba)Cl]·CH$_3$OH (2). A mixture of ZnCl$_2$ (14 mg, 0.1 mmol), 4-Hbta (19 mg, 0.1 mmol), and MeOH (5 mL) was placed in a Teflon-lined stainless steel vessel (15 mL) and heated at 120 °C for 3 days and then cooled to room temperature at a rate of 5°C/h. Colorless, needle-like crystals were collected by filtration, washed with MeOH and dried in air to afford 22 mg (70% based on 4-Hbta) of product. Anal. Calcd. for C$_{10}$H$_{10}$ClN$_3$O$_3$Zn: C, 37.41; H,

3.14; N, 13.09. Found: C, 37.45; H, 3.12; N, 13.12. IR (cm-1, KBr): 3442(m, br), 3116(w), 1710(w), 1608(s), 1535(s), 1459(s), 1379(s), 1237(m), 1178(w), 1095(m), 1016(m), 866(w), 781(m), 696(w), 624(w), 527(w).

2.2.3. Synthesis of [Zn(4-tba)$_2$] (3). A mixture of ZnCl$_2$ (14 mg, 0.1 mmol), 4-Htba (19 mg, 0.1 mmol), and DMF (5 mL) was placed in a Teflon-lined stainless steel vessel (15 mL) and heated at 120 °C for 3 days and then cooled to room temperature at a rate of 5°C/h. Colorless, block crystals were collected by filtration, washed with MeOH and dried in air to afford 10 mg (45% based on 4-Htba) of **3**. Anal. Calcd. for C$_{18}$H$_{12}$N$_6$O$_4$Zn: C, 48.94; H, 2.74; N, 19.03. Found: C, 48.92; H, 2.76; N, 19.00. IR (cm^{-1}, KBr): 3447(br, m), 3118(m), 1633(s), 1581(m), 1531(s), 1366(s), 1235(m), 1095(m), 1034(s), 1015(m), 842(m), 780(m), 696(w), 655(w), 506(w).

2.2.4. Synthesis of [Zn(4-tba)$_2$]·DMA·3.5H$_2$O (4). A mixture of ZnCl$_2$ (14 mg, 0.1 mmol), 4-Htba (19 mg, 0.1 mmol), and DMA (5 mL) was placed in a Teflon-lined stainless steel vessel (15 mL) and heated at 95 °C for 3 days and then cooled to room temperature at a rate of 5°C/h. A little of colorless, block crystals were collected by filtration, washed with ether and dried in air to afford 11 mg (38% based on 4-Htba) of **4**. Anal. Calcd. for C$_{22}$H$_{28}$N$_7$O$_{8.5}$Zn: C, 44.64; H, 4.77; N, 16.57. Found: C, 44.62; H, 4.79; N, 16.54. IR (cm-1, KBr): 3220(br, m), 3106(m), 1607(s), 1529(s), 1398(s), 1313(w), 1243(m), 1098(m), 1010(m), 865(m), 782 (m), 705(w), 625 (w), 566 (m). The framework of **4** can also be obtained by another procedure as follows: the resulting colorless filtrate after the synthesis of **3** was allowed to stand at room temperature, and slowly evaporated in air for over two weeks to give colorless block crystals of the framework of **4** (yield:40% based on 4-Htba). Elemental and thermal gravimetric analyses reveal that the molecular formula synthesized by this method is [Zn(4-tba)$_2$]·0.5DMF·2H$_2$O (**4'**).

2.2.5. Synthesis of [Cd(4-tba)$_2$]·DMF·3.6H$_2$O (5). A mixture of Cd(NO$_3$)$_2$·4H$_2$O (31 mg, 0.1 mmol), 4-Htba (19 mg, 0.1 mmol) and DMF (5 mL) was placed in a Teflon-lined stainless steel vessel (15 mL) and heated at 95 °C for 3 days and then cooled to room temperature at a rate of 5°C/h. Colorless, block crystals were collected by filtration, washed with ether and dried in air to afford 19 mg (62% based on 4-Htba) of product. Anal. Calcd. for C$_{21}$H$_{26.2}$CdN$_7$O$_{8.6}$: C, 40.25; H, 4.21; N, 15.65. Found: C, 40.20; H, 4.25; N, 15.68. IR (cm^{-1}, KBr): 3289(br, m), 3099(m), 1632(m), 1607(s), 1538(s), 1409(s), 1305(w), 1248(m), 1092(m), 1009(w), 860(m), 783(m), 696(w), 519(m).

2.2.6. Synthesis of [Cd(4-tba)$_2$] (6). A mixture of Cd(NO$_3$)$_2$·4H$_2$O (31 mg, 0.1 mmol), 4-Hbta (19 mg, 0.1 mmol), 4,4'-bipyridine (16 mg, 0.1 mmol), DMF (4 mL), and MeOH (1 mL) was placed in a Teflon-lined stainless steel vessel (15 mL) and heated at 120°C for 3 days and then cooled to room temperature at a rate of 5°C/h. Colorless, block crystals were collected by filtration, washed with EtOH and dried in air to afford 8 mg (32% based on 4-Htba) of product. Anal. Calcd. for C$_{18}$H$_{12}$CdN$_6$O$_4$: C, 44.23; H, 2.47; N, 17.20. Found: C, 44.20; H, 2.51; N, 17.22. IR (cm^{-1}, KBr): 3384(br, m), 3105(m), 1607(s), 1541(s), 1408(s), 1313(m), 1248(m), 1092(m), 1034(w), 856(m), 784(m), 696(w), 625(w), 510(m).

2.2.7. Synthesis of [Cd$_5$Cl$_4$(4-tba)$_6$]·1.5DMF·4H$_2$O (7). A mixture of CdCl$_2$·2.5H$_2$O (23 mg, 0.1 mmol), 4-Htba (19 mg, 0.1 mmol) and DMF (3 mL), CH$_3$CN (1 mL) was heated at 95 ^{o}C for 3 days under autogenous pressure. The mixture was slowly cooled to room temperature at a rate of 5 ^{o}C/h. Colorless block crystals were collected by filtration, washed with EtOH and dried in air to afford 5 mg (15% based on 4-Htba) of product. Anal. Calcd. for C$_{58.5}$H$_{54.5}$Cd$_5$Cl$_4$N$_{19.5}$O$_{17.5}$: C, 34.88; H, 2.73; N, 13.56. Found: C, 34.95; H, 2.80; N, 13.61. IR (cm^{-1}, KBr): 3544(br, m), 3120(m), 1631(m), 1603(s), 1561(s), 1538(s), 1388(s), 1360(m), 1260(s), 1092(m), 862(m), 783(m), 691(w), 642(w), 510(m).

2.3. X-ray crystallograpy

Diffraction intensities of the seven compounds were collected on a Bruker Apex CCD diffractometer or on a Rigaku R-AXIS SPIDER diffractometer with graphite-monochromated Mo Kα radiation (λ = 0.71073 Å). Absorption corrections were applied by using multi-scan program SADABS[17] or the program ABSCOR.[18] The structures were solved with direct methods and refined with a full-matrix least-squares technique with the SHELXTL program package.[19] Anisotropic thermal parameters were applied to all non-hydrogen atoms. All the hydrogen atoms were generated geometrically expect for the hydrogen atoms of the disordered water molecules in **7**. Due to the presence of large cavities in the structure and heavily disordered solvent molecules in the cavities, the crystals of **4** and **5** scattered weakly and only low-angle data could be detected. An attempt to locate and refine the solvent molecules failed. Thus, the SQUEEZE routine of PLATON was applied for **4** and **5** to remove the contributions to the scattering from the solvent molecules.[20] The reported refinement is of the guest-free structure using the *.hkp file produced by the SQUEEZE routine. Crystal data and structure refinement are summarized in Table S1. The void

Table 1 Crystal data for **1**-**7**

Compound	1	2	3	4
Empirical formula	$C_{18}H_{16}N_6O_6Zn$	$C_{10}H_{10}ClN_3O_3Zn$	$C_{18}H_{12}N_6O_4Zn$	$C_{22}H_{28}N_7O_{8.5}Zn$
Formula weight	477.74	321.03	441.71	591.89
Crystal system	Monoclinic	Monoclinic	Monoclinic	Orthorhombic
Space group	$C2/c$	$P2_1/c$	$C2$	$Pbcn$
a (Å)	13.519(2)	9.097(3)	13.664(2)	20.0621(18)
b (Å)	9.8960(17)	17.622(5)	7.8616(13	15.5930(14)
c (Å)	14.609(2)	7.464(2)	8.2311(14)	17.2349(15)
α (°)	90	90	90	90
β (°)	112.259(3)	92.337(6)	91.400(3)	90
γ (°)	90	90	90	90
V (Å³)	1808.9(5)	1195.6(6)	883.9(3)	5391.6(8)
Z	4	4	2	8
D_c (g cm⁻³)	1.754	1.784	1.660	1.458
μ (mm⁻¹)	1.413	2.280	1.430	0.971
R_{int}	0.0201	0.0392	0.0296	0.0503
GOF	1.123	1.126	1.012	1.012
R_1 [$I > 2\sigma(I)$]	0.0432	0.0505	0.0390	0.0441
wR_2 [all data]	0.1210	0.1322	0.0755	0.1143

Compound	5	6	7
Empirical formula	$C_{21}H_{26.2}CdN_7O_{8.6}$	$C_{18}H_{12}CdN_6O_4$	$C_{58.5}H_{54.5}Cd_5Cl_4N_{19.5}O_{17.5}$
Formula weight	626.69	488.74	2014.55
Crystal system	Orthorhombic	Orthorhombic	Triclinic
Space group	$Pnc2$	$Fdd2$	P-1
a (Å)	8.3848(17)	16.680(3)	12.946(3)
b (Å)	14.808(3)	32.764(7)	17.321(3)
c (Å)	11.494(2)	6.5537(13)	22.153(4)
α (°)	90	90	70.13(3)
β (°)	90	90	76.08(3)
γ (°)	90	90	73.31(3)
V (Å³)	1427.1(5)	3581.8(12)	4418.3(15)
Z	2	8	2
D_c (g cm⁻³)	1.458	1.813	1.508
μ (mm⁻¹)	0.791	1.260	1.370
R_{int}	0.0295	0.0299	0.0598
GOF	1.074	1.199	1.020
R_1 [$I > 2\sigma(I)$]	0.0284	0.0176	0.0545
wR_2 [all data]	0.0779	0.0522	0.1700

$R1 = \sum||F_o| - |F_c||/\sum|F_o|$. $wR_2 = [\sum w(F_o^2 - F_c^2)^2/\sum w(F_o^2)^2]^{1/2}$

volume (excluding guest solvent molecules) in the crystal cell was calculated using the program PLATON.[20] Crystal data as well as details of data collection and refinements for the complexes are summarized in Table 1.

3. Result and discussion

(a)

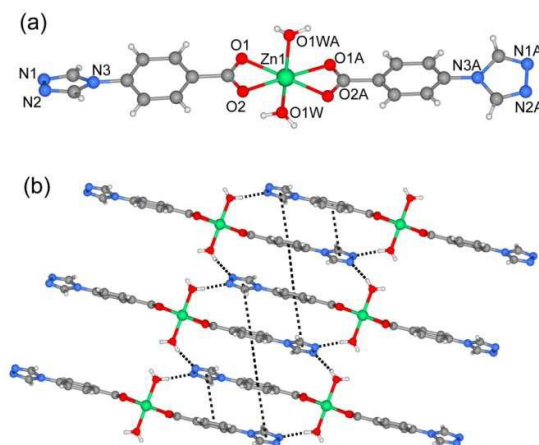(b)

CrystEngComm Accepted Manuscript

Fig. 1 (a) The coordination environment of the zinc atoms in **1** and only one position of disordered water molecules are shown for clarity. Symmetric codes: A: -x, y, 1/2-z. (b) 2D supramolecular network of **1** along the *b*-axis constructed by hydrogen bonds.
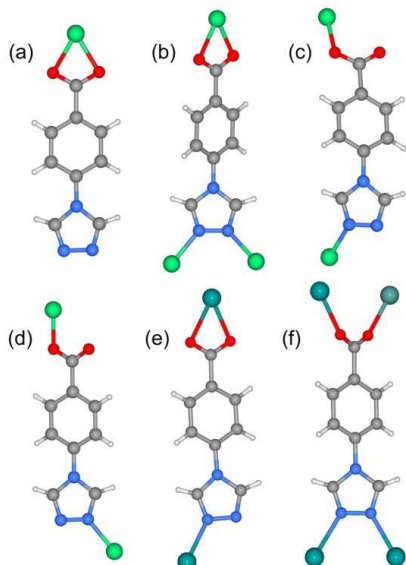

Fig 2 (a-g) The coordination environment of 4-tba ligands in complexes **1**-**7**.

3.1 Crystal structure of [Zn(4-tba)$_2$(H$_2$O)$_2$] (1). Single-crystal X-ray analysis reveals that complex **1** shown a 0D mononuclear structure, and is isomorphous to the previously reported complexes constructed by the first-transition metal ions (such as, Mn^{2+}, Co^{2+} Ni^{2+}, Cu^{2+}and Cd^{2+}) and 4-tba anions.[16a,21] As shown in Fig. 1a, the asymmetric unit contains a half molecule of [Zn(4-tba)$_2$(H$_2$O)$_2$], and a crystallographic mirror plane passes through the Zn1 site. The Zn1 adopts an octahedral coordination geometry, being coordinated by four oxygen atoms from two different 4-tba ligands and two coordinated water molecules. In complex **1**, the deprotonated 4-tba ligand coordinates with Zn^{II} ions in a O,O-chelating mode, and the nitrogen atoms from 4-tba ligand are not coordinated to the metal atoms (Fig. 2a). However, the uncoordinated nitrogen atoms from 4-tba anions (N1 and N2) are involved in two intermolecular O–H⋯N hydrogen bonds (O⋯N = 2.746(17)-2.790(17) Å, H⋯N = 2.04-2.06 Å, O-H⋯N = 155.8-164.5°) with two neighbouring coordinated water molecules to generate a
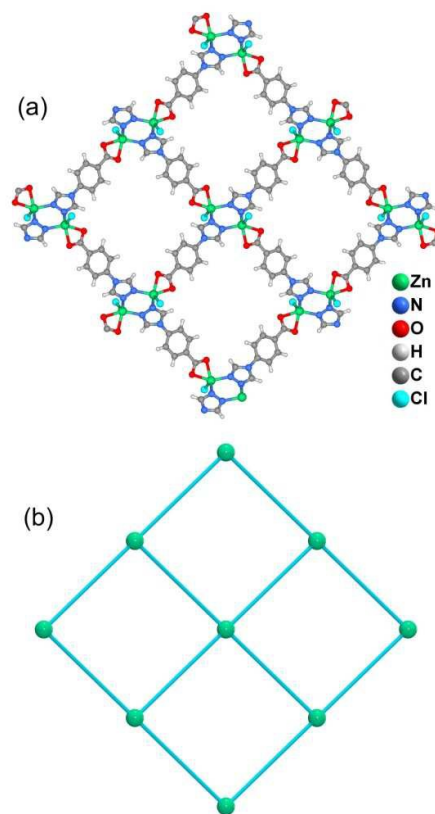

Fig. 3 (a) The two-dimensional network of **2**. (b) The 4^4-sql net of **2**.

2D supramolecular structure (Fig. 1b). The corresponding hydrogen bonding parameters are summarized in Table S1†. Moreover, the π–π interactions between 4-bta further stabilize the 2D supramolecular layer (closet interplanar and centroid-centrioid separations are in 3.34-3.78 and 3.87-4.13 Å, respectively). These 2D layers are further assembled by the C–H⋯O weak interactions (C⋯O = 3.295(15)-3.329(4) Å, H⋯O = 2.40-2.49 Å, C-H⋯O= 145.3-174.3°) between adjacent layers into an infinite 3D supramolecular structure (Fig. S8†).

3.2 Crystal structure of [Zn(4-tba)Cl]·CH$_3$OH (2). When MeOH was utilized as the reaction solvent in place of water under similar synthetic conditions in **1**, a new complex **2** with a different structure was isolated. Compound **2** crystallizes in the monoclinic space group *P*21/*c*, and exhibits a two-dimensional (2D) layer. As depicted in Fig. S9†, each Zn1 is five-coordinated with two N atoms from two 4-tba ligands, two oxygen atoms from one chelating carboxylate group and one chloride ion to form a highly distorted square-pyramidal coordination geometry (trigonality index τ = 0.39).[22] The chloride ion only acts as an auxiliary ligand in a monodentate coordination mode, while each 4-tba ligand adopts μ_3-bridging fashion to connect three zinc(II) ions through two N atoms from the triazolyl group and two O atoms from one carboxylate group with μ_1-η^1:η^1 chelating mode (Fig. 2b). The Zn ions are linked together by 4-tba in μ_3-η^1:η^1:η^1:η^1 mode to generate 2D network with 3-connected 4.8^2 topology when Zn and 4-tba are regarded as two kinds of 3-connected nodes (Fig. S10†). If

ARTICLE   Journal Name

the dinuclear [Zn$_2$(triazole)$_2$] subunit is further simplified as 4-connecting nodes and the 4-tba ligands as linkers, compound **2** has a simple 4^4-sql network (Fig. 3b). The 2D layers are further linked together via intermolecular week C-H···O hydrogen bonds (C···O = 2.965(6)-3.496(7) Å, H···O = 2.25-2.57 Å, C-H···O= 112.8-171.5^o) to generate a 3D structure (Fig. S11†). Furthermore, the π–π stacking interactions between the adjacent benzene ring rings (closet interplanar and centrioid-centrioid separations are in 3.36 and 3.78 Å, respectively) may further stabilize the structure (Fig. S12†).

3.3 Crystal structure of [Zn(4-tba)$_2$] (3). When DMF was utilized as the reaction solvent in place of water or MeOH

under similar synthetic conditions in **1** and **2**, complex **3** was obtained. Compound **3** is crystallized in the chiral space group C2, as a result of the unsymmetrical nature of organic ligand. There are one half of Zn^{2+} ion and one tba ligand in the asymmetric unit. As shown in Fig. 4a, the zinc ion (Zn1) is sited on the crystallographic C2 axis, and adopts a tetrahedral coordination geometry, being coordinated by two oxygen atoms from two symmetry related 4-tba ligands and two nitrogen atoms from other two 4-tba ligands. The 4-tba ligand acts as an unsymmetic, bidentate, linear linker (Fig. 2c), and each Zn(II) atom is connected to four adjacent Zn(II) atoms
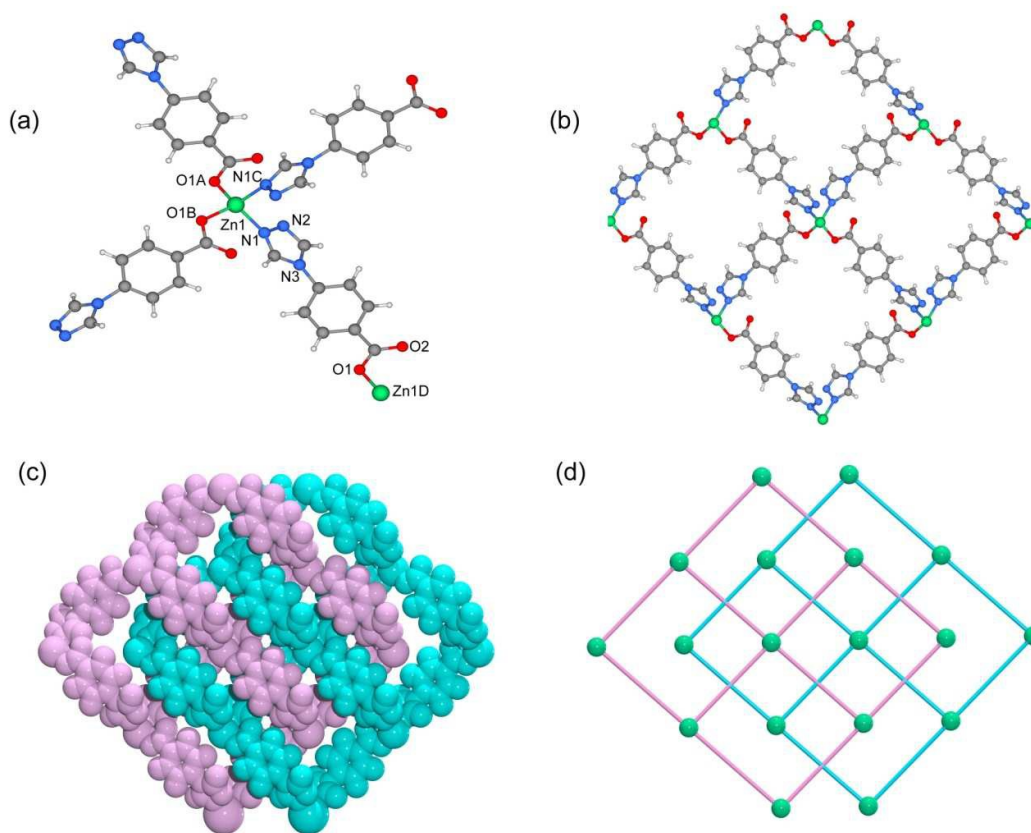

Fig. 4 (a) The coordination environment of the zinc atoms and 4-tba ligand in **3**. Symmetric codes: A: x, y-1, z+1; B: -x+2, y-1, -z-2; C: -x+2, y, -z-1. (b) A single 2D layer structure of **3**. (c) Space-filing diagram of the 2-fold interpenetrating framework of **3**. (d) Topological representation of the 2-fold interpenetration in **3**.
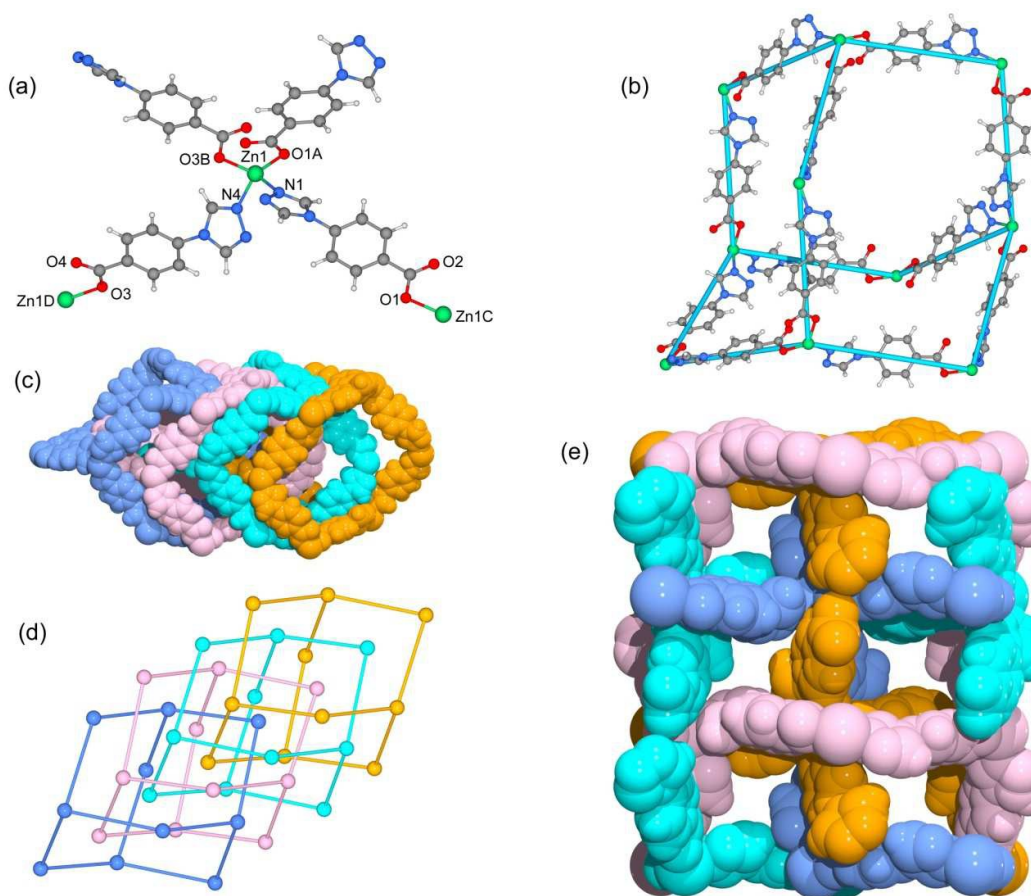
Fig. 5 (a) The coordination environment of the zinc atoms and 4-tba ligands in **4**. Symmetric codes: A: x-1/2, -y+1/2, -z+2; B: -x+1/2, -y-1/2, z+1/2; C: x+1/2, -y+1/2, -z+2; D: -x+1/2, -y-1/2, z-1/2. (b) A single diamond motif in **4**. (c) Space-filing diagram of the 4-fold interpenetrating adamantanoid cages in **4**. (d) Topological representation of the 4-fold interpenetration in **4**. (e) Space-filing diagram of 3D framework of **4** viewed along the *b*-axis.

through the four linear 4-tba linkers to result in a 4^4-sql 2D network. Each 2D layer has the effective square window with the dimension of ca. 5.0 Å^2 (Fig. 4b). Moreover, each 2D layer has enough "empty" space to allow another 2D layer to interpenetrate and form a two-fold parallel interwoven net (Fig. 4c and d), making **3** a nearly dense structure with the total solvent-accessible volume only comprising 2.1% (18.7 Å^3) of the crystal volume.[20] Furthermore, the π−π stacking interactions can also be observed in **3** between the benzene rings from adjacent two-dimensional layers (Fig. S13†, closet interplanar and centrioid-centrioid separations are in 3.51 and 3.66 Å, respectively).

3.4 Crystal structure of [Zn(4-tba)$_2$]·DMA·3.5H$_2$O (4). Although the framework of the compound **4** has been previously reported, it needs triethylamine and HNO$_3$ as the raw reaction materials.[16a] Herein, the framework of **4** can be prepared by slow evaporation of the filtrate of **3** or by using DMA as reaction solvent at 95 °C. Compound **4** crystallizes in orthorhombic system, space group *Pbcn*. The asymmetric unit contains one Zn^{2+} ion and two tba ligands. Being Similar to **3**, the Zn(II) atom is also four-coordinated with two oxygen atoms from two symmetry related 4-tba ligands and two nitrogen

atoms from other two 4-tba ligands (Fig. 5a). Although the 4-tba ligands also act as bidentate, linear linkers, they adopt different coordination geometries (Fig. 2d) with the oxygen and nitrogen in different orientation. Each Zn(II) atom is connected to four adjacent Zn(II) atoms through the four linear 4-tba linkers to result in a 3D diamond-like framework with the point symbol 6^6 and the long symbol $6^2 \cdot 6^2 \cdot 6^2 \cdot 6^2 \cdot 6^2 \cdot 6^2$, typical of a dia topology, containing large adamantanoid cages (Fig. 5b). The Zn···Zn distances separated by 4-tba ligands are 12.21 and 12.28 Å, respectively, and the Zn··Zn···Zn angles range from 89.77° to 119.60°, which is a significant deviation from the 109.5° expected for an idealized diamond network. A single adamantanoid framework possesses a large cavity and causes four independent equivalent cages to interpenetrate with each other (Figure 5c and d). The interpenetration mode of the four independent nets is the so-called "normal" type for diamondoid frames, which belongs to class Ia. Despite even 4-fold interpenetration, **4** displays a 1D porous framework with rhombic channels along the *b*-axis (Fig. 5e and Fig. S14†, effective aperture is 2.2 × 2.9 Å^2). The total void value of the channel is estimated to be 2136.8 Å^3, approximately 39.6% of the total crystal volume of 5391.6 Å^3.

3.5 Crystal structure of [Cd(4-tba)$_2$]·DMF·3.6H$_2$O (5). Heating a mixture of Cd(NO$_3$)$_2$·4H$_2$O and 4-Hbta in DMF (5 mL) at 95 °C for 72 h afforded pure-phase **5** as colorless block crystals. Compound **5** crystallizes in orthorhombic system, space group *Pnc*2, and the asymmetric unit contains one half of Cd^{2+} ion and one tba ligand as shown in Fig. 6a. In **5**, the Cd1 center with O4N2 binding set is coordinated by two pairs of oxygen atoms of chelating carboxylate groups from two symmetry related 4-tba ligands and two N atoms from other two 4-tba ligands (Figure 6a), displaying a highly distorted octahedral coordination sphere. Each 4-tba ligand exhibits μ_2-coordination modes to connect two cadmium(II) ions through one N atom from the triazolyl group and two O atoms from one carboxylate group with μ_1-η^1:η^1 chelating mode (Fig. 2e). Given that the chelating carboxylates are treated as one connecting point, each Cd(II) atom is connected to four adjacent Cd(II) atoms through the four linear 4-tba linkers to result in an uninodal 3D 4-connected dia (6^6) topology (Fig. S15†). The Cd···Cd distances separated by 4-tba ligand are 12.58 Å, and the Cd···Cd···Cd angles range from 96.37° to 125.61°, which is a significant deviation from the 109.5° expected for an idealized diamond network. The single 3D network also consists of large windows, which are filled via mutual interpenetration of four independent equivalent networks (Fig. 6b). Interestingly, the mode of interpenetration is different from the normal mode and may be described as two sets of normal 2-fold nets, that is, an unusual [2 + 2] mode of interpenetration (Fig. 6c). An analysis of the topology of interpenetration according to recent classification reveals that this interpenetration in **5** belongs to Class IIIa.[23] To the best of our knowledge, among those unusual interpenetrating examples, 4-fold interpenetrating dia MOFs with [2 + 2] mode are relatively scarce.[24] Despite even 4-fold interpenetration, **5** still possesses large square channels with an effective pore diameter 6.4 Å along the *a* direction (Fig. 6d and Fig. S16†). The total void value of the channel is estimated to be 628.7 Å^3, approximately 44.1% of the total crystal volume of 1427.1 Å^3.

3.6 Crystal structure of [Cd(4-tba)$_2$] (6). Heating a mixture of Cd(NO$_3$)$_2$·4H$_2$O, 4-Hbta and 4,4'-bipyridine in the mixed solvent of DMF/MeOH at 120 °C afforded colorless block crystals of **6**. Compound **6** exhibits a 5-fold interpenetrated dia topological net. In contrast to **5**, **6** crystallizes in orthorhombic space group *Fdd*2, rather than *Pnc*2 in **5** (Table 1). Being similar to **5**, the asymmetric unit also contains one half of Cd^{2+} ion and one tba ligand (Fig. 7a) and each Cd atom is also coordinated by two pairs of oxygen atoms of chelating carboxylate groups from two symmetry related 4-tba ligands and two N atoms from

Fig. 6 (a) The coordination environment of the cadmium atoms and 4-tba ligands in **5**. Symmetric codes: A: -x+1, -y, z; B: x+1, -y-1/2, z-1/2; C: -x, y+1/2, z-1/2; D: x-1, -y-1/2, z+1/2. (b) Space-filing diagram of the 4-fold interpenetrating adamantanoid cages in **5**. (d) Topological representation of the 4-fold interpenetration in **5**. (e) Space-filing diagram of 3D framework of **5** viewed along the *b*-axis.
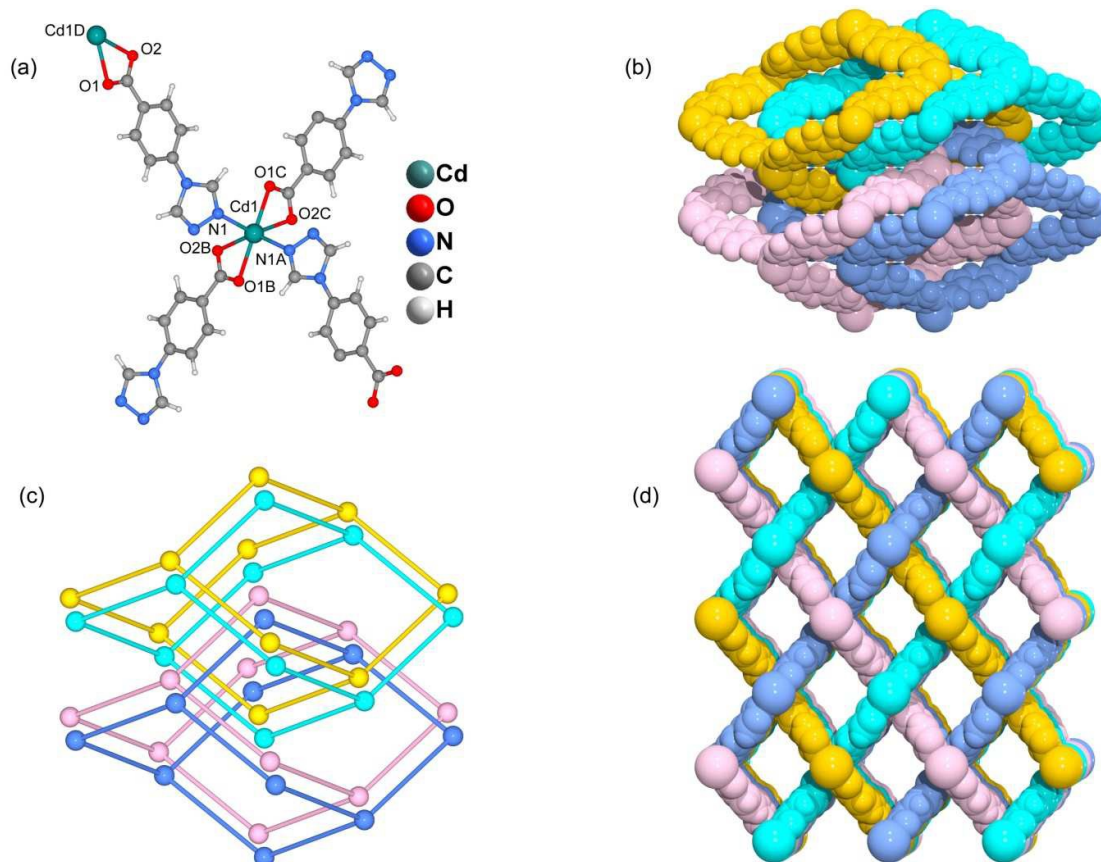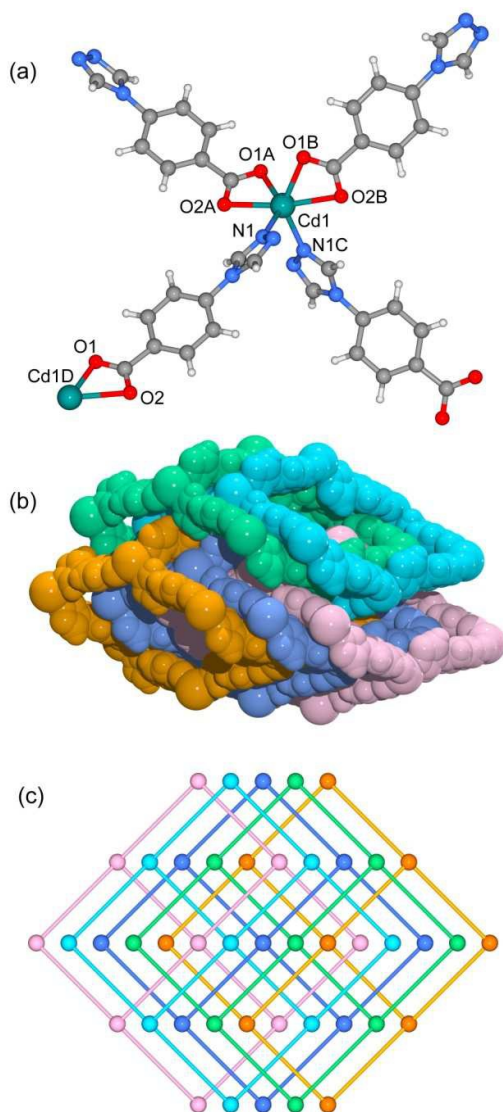
CrystEngComm

ARTICLE

Fig. 7 (a) The coordination environment of the cadmium atoms and 4-tba ligands in **6**. Symmetric codes: A: x-1/4, -y+1/4, z-5/4; B: -x+1/4, y-1/4, z-5/4; C: -x, -y, z; D: x+1/4, -y+1/4, z+5/4. (b) Space-filing diagram of the 5-fold interpenetrating adamantanoid cages in **6**. (c) Topological representation of the 5-fold interpenetration in **6**.

other two 4-tba ligands. Although each 4-tba ligand in **6** adopts the coordination modes (Fig. 2e) similar to that of **5**, the dihedral angle between the benzene ring and triazole ring in **6** (46.13°) is much larger than that of **5** (19.98°). As shown in Fig. 17†, each Cd(II) atom is also connected to four adjacent Cd(II)

atoms through the four linear 4-tba linkers to result in a 3D 4-connected dia (6^6) topology. Notably, the large adamantanoid cages in a single dia network are much distorted than those of **4** and **5**, in which the Cd···Cd distances separated by 4-tba ligand are 12.31 Å, and the Cd···Cd···Cd angles range from 96.58° to 140.41°. As illustrated in Figure 7b, the single framework of **6** is interpenetrated by four identical dia nets, giving rise to the final 5-fold interpenetrated dia framework. Being different from **5**, the interpenetrating fashion in **6** with TOPOS suggests the so-called 'normal' type for diamondoid frames, which belongs to class Ia with the interpenetration vector being equal to the *c* axis (6.55 Å). Due to 5-fold interpenetration, **6** is a dense structure with no residual solvent accessible area in unit cell.

3.6 Crystal structure of [Cd₅Cl₄(4-tba)₆]·1.5DMF·4H₂O (7). When CdCl₂·2.5H₂O instead of Cd(NO₃)₂·4H₂O and the mixed solvent of DMF/CH₃CN in place of DMF under similar synthetic conditions in **5**, a different structure was formed for **7**. Compound **7** crystallizes in the triclinic space group *P*-1. As shown in Fig 8a, there are five crystallographically independent Cd(II) ions in an asymmetric unit with distorted octahedral coordination geometries. A notable feature in the structure of **7** is that 4-tba ligands exhibit four coordination modes existing together in one compound: (i) It acts as a bidentate linkage, using one N atoms and one oxygen atom to bridge two Cd(II) ions (Fig. 2d); (ii) It also acts as a bidentate linkage, using one N atoms to bridge one Cd(II) ion and two oxygen atoms to chelate one Cd(II) ion (Fig. 2e); (iii) It takes μ_3-brdiging modes by using two N atoms to bridge two Cd(II) ions and two oxygen atoms to chelate one Cd(II) ion (Fig. 2b); (iv) It exhibits μ_4-brdiging modes to bridging four Cd(II) ions where the carboxylate group bridge two adjacent Cd(II) ions in bis-monodentate syn-syn mode (Fig. 2f). Also interesting is the decanuclear cadmium-chloride chain unit linked by μ_2-chloride and μ_3-chloride (Fig. 8b). As shown in Fig. 8c and 8d, the decanuclear cadmium-chloride units are linked by the 4-tba ligands with four different coordination modes into a 3D framework with 2D channels in which DMF and water solvates reside. The channels are rectangle with the size of 2.01 × 4.52 Å² along the *a*-axis, whereas the channels along the *c*-axis are dumbbell shaped with the effective aperture of 2.45 ×6.38 Å². The cavity volume is estimated to be ca. 38.4% of the total crystal volume, calculated using the PLATON program after guest removal. When μ_2-chloride and μ_3-chloride are regarded as a rod and 3-connected node, respectively, and the 4-tba ligands are regarded as 2, 3, 4-connected nodes, the 3D structure of **7** can be rationalized as an unusual 10-nodal (3,3,3,4,4,4,5,6,6,6)-connected topology (Fig. S18†).
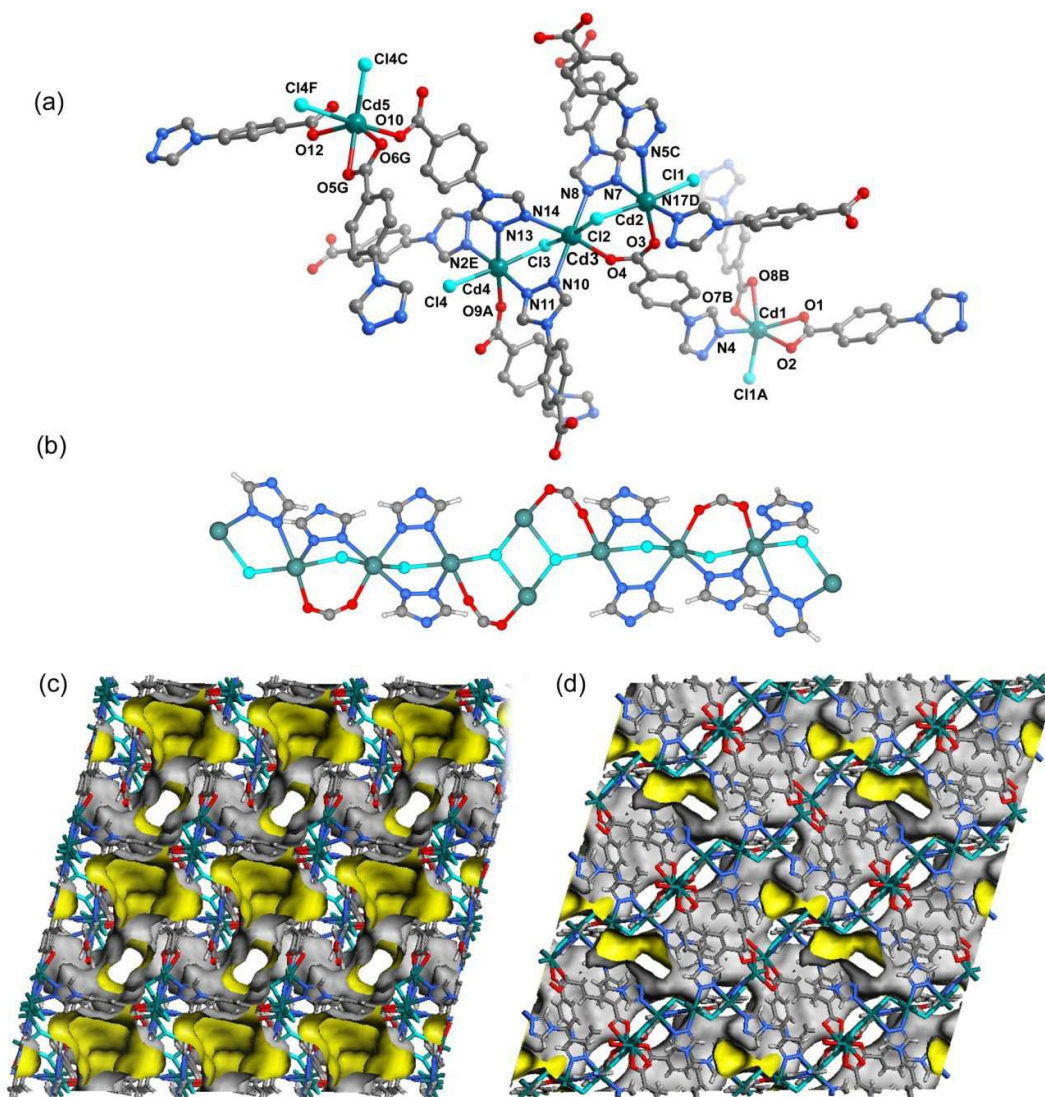
CrystEngComm

ARTICLE

Fig. 8 (a) The coordination environment of the cadmium atoms in **7** and the hydrogen atoms are omitted for clarity. Symmetric codes: A: x+1, y, z; B: x+1, y-1, z; C: x-1, y, z; D: x+1, y, z-1; E: x-1, y, z+1; F: -x-1, -y+2, -z+1; G: x-1, y+1, z. (b) The decanuclear cadmium-chloride chain unit linked by μ_2-chloride and μ_3-chloride in **7**. (c) Views of the 3D framework and channel structure of **7** along the *c*-axis.(d) Views of the 3D framework and channel structure of **7** along the *a*-axis.

3.7 Synthesis of the Complexes and Comparison of the Structures. Compounds **1**-**7** were synthesized under hydro/solvothermal conditions. In general, the reaction variables (solvent, metal salts species, concentration, temperature, and *p*H value, anion, etc.) can influence the reaction process and the final products. Solvent as template is one of the keys to the construction of metal complexes because solvent can act as space-filling molecules.[9] Complexes **1**-**3** with different structures were

obtained under the same reaction conditions by using different reaction solvent. Besides the solvent effect, reaction temperature is another key factor in controlling the topology and dimensionality of the frameworks by thermal desolvation and changing the coordination modes. The mononuclear structure of **1** and dense structures of **2**, **3** and **6** were obtained at 120 °C, while porous structures **4**, **5** and **7** were crystallized at a low temperature of 95 °C. Moreover, the

framework of **4** can also be obtained by slow evaporation of the filtrate of **3** (verified by PXRD, Fig S4†), which demonstrates that the concentration also influences the formation of **3** and **4**. It should be pointed that 4,4'-bipyridine plays a key role in the synthesis of **6**, and it cannot be obtained without 4,4'-bipyridine. Thus, 4,4'-bipyridine may be act as a weak base to deprotonate 4-Htba and provide automatic control of the acid/base balance of the solution. Comparing **5** with **7**, we find that the anion also influences the formation of the network besides the solvent effect, and the chloride anion from $CdCl_2 \cdot 2.5H_2O$ can involve in coordinating metal ions. Also, the nature of different metal centers is a key factor to construct diverse frameworks, and different coordination geometry around Zn^{II}/Cd^{II} centers resulted in completely different structures for two series of Zn^{II}/Cd^{II} complexes **1**-**7**. Compared to the ionic radius of Zn(II) ion (74 pm), that of disparate Cd(II) metal ion (97 pm) is relatively larger; as a result it has tendency to adopt higher coordination numbers to accommodate more bulkiness in its coordination sphere, thereby forming complicated or higher dimensional structures.

Table 2 Dihedral angles between benzene ring and triazole ring in 1-7

Compound	$\alpha /°$	Coordination modes
1	24.84	(a)
2	41.70	(b)
3	40.34	(c)
4	39.56, 42.35	(d)
5	19.98	(e)
6	46.13	(e)
7	28.26-50.53	(b), (d)-(f)

On the other hand, the 4-Htba ligand involving bifunctional groups of carboxylate and triazolyl can exert diverse coordination modes as shown in Fig. 2. The carboxylate group of 4-Htba in all complexes are deprotonated to give 4-tba anion to ligate with bivalent metal ion. The benzene ring and triazole ring in 4-tba anion ligand could freely rotate along the C–N bonds to adjust themselves to match with the coordination preferences. The dihedral angles α between benzene rings and triazole rigns were calculated and compiled in Table 2. As is well known, the different coordination modes of 4-tba ligand always bring different dihedral angles α. For example, the dihedral angles α in complexes **1-4** can range from 24.84 to 42.35°. However, although the 4-tba ligands in **5** and **6** takes the similar coordination modes (Fig.2e), the dihedral angles α can be largely different due to the different crystal packing modes: **5** is a [2 + 2] interpenetrating dia net belonging to Class IIIa, whereas **6** is 5-fold interpenetrating dia net of Class Ia). The compound **5** show the smallest dihedral angles α in all the complexes **1-7**. Furthermore, the π–π stacking interactions in these compounds also vary differently. Compound **1-3** possess significant offset face-to-face π–π stacking interactions, whereas there are almost negligible aromatic stacking interactions existing in **4-7** because their long centroid–centroid distances are beyond to
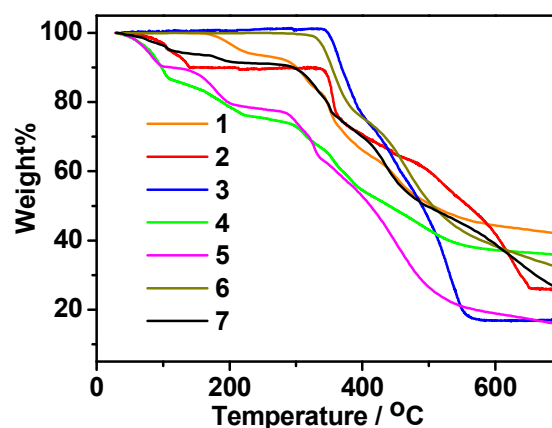

Fig. 9 TG curves of **1**-**7** in N_2.

4.0 Å (Table S2†).

3.8 X-ray powder diffraction (PXRD) and thermal analysis (TG)

In order to confirm the phase purity of these compounds, powder X-ray diffraction (PXRD) patterns of **1-7** were obtained at room temperature. As shown in Fig. S1-S7†, the peak positions of the theoretical and experimental PXRD patterns are in agreement with each other, indicating single phases of **1**-**7** are formed.

Thermogravimetric analyses (TGA) were carried out to study the thermal stabilities of **1–7**. As shown in Fig. 9, In general, the mononuclear structure of **1** and the porous structures of **4**, **5** and **7** can be stable below 280 °C. The 2D structure of **2** and the dense structures of **3** and **6** can be stable up to 315 °C, and thus are much more stable than the mononuclear structure (**1**) and the porous structures (**4**, **5** and **7**). In the TG curve of **1**, coordinated water molecules were lost from 100 to 275 °C (calcd.: 7.54%, found: 7.49%). Above 275 °C, the sample suffered an abrupt weight loss, indicating the collapse of the remaining substance. For **2**, the lattice methanol molecules were released from 40 to 145 °C (calcd.: 9.98%, found: 10.17%). The remaining substance is stable upon heating to 325 °C, and then the gradual and rapid weight decrease happened. For **3**, it can be stable under 335 °C and decomposed at higher temperature. For **4**, the weight loss of 25.32% at temperatures below 270 °C is consistent with the removal of one molecules of DMA and 3.5 molecules of H_2O per formula unit (calcd.: 5.37%), and the further weight loss indicates the decomposition of the framework from 280 °C. For **5**, the weight loss of 22.05% at temperatures below 250 °C is consistent with the removal of one molecules of DMF and 3.6 molecules of H_2O per formula unit (calcd.: 22.01%). In the case of compound **6**, no obvious weight loss was observed until the temperature rose to 315 °C. The TG curve of **7** shows a steady weight loss of water and DMF molecules below 250 °C (observed: 8.90%, calculated: 9.02%), and the remaining substance begins to decompose from 274 °C.
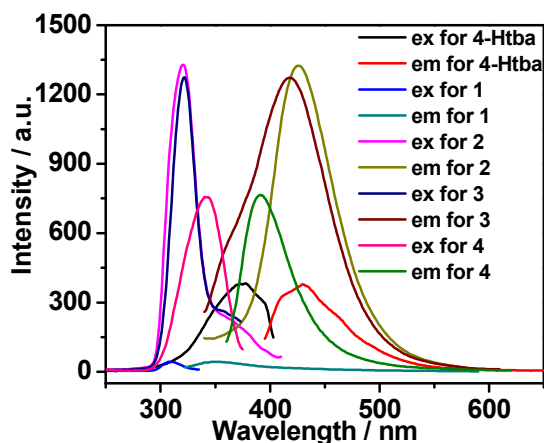
ARTICLE

Journal Name

Fig. 10 The excitation and emission spectra of Zn(II) complexes **1–4** in solid state at room temperature (excitation slit: 2.5, emission slit: 1.0).

2.9 Photoluminescent properties

Luminescent MOFs with d^{10} metal ions are of great interest due to their various applications in photochemistry, chemical sensors and light emitting diodes. Therefore, the solid-state luminescence of free ligands Hbta and the compounds **1**-**7** are investigated at room temperature, as depicted in Fig. 10, Fig. 11 and Table 3. The main emission peaks of the 4-Hbta were observed at 427 nm (λ_{ex} = 377 nm), which can be assigned to the $\pi^* \rightarrow n$ or $\pi^* \rightarrow \pi$ transitions.[24] The compounds **1**-**7** emit purple or bluish-purple emission with maximum emission peaks at 351 nm, 426 nm, 418 nm, 391 nm, 400 nm, 425nm and 429 nm if excited at 309 nm, 321 nm, 322 nm, 343 nm, 353 nm, 324 nm, and 369 nm, respectively. Since the Zn(II) and Cd(II) ions are difficult to oxidize or reduce due to their d^{10} configurations, the emission of these complexes is neither metal-to-ligand charge transfer (MLCT) nor ligand-to-metal charge transfer (LMCT) in nature. Thus, the emission of **1**-**7** is probably attributed to the intraligand transitions modified by metal coordination. In contrast to the free ligand (4-Htba), the
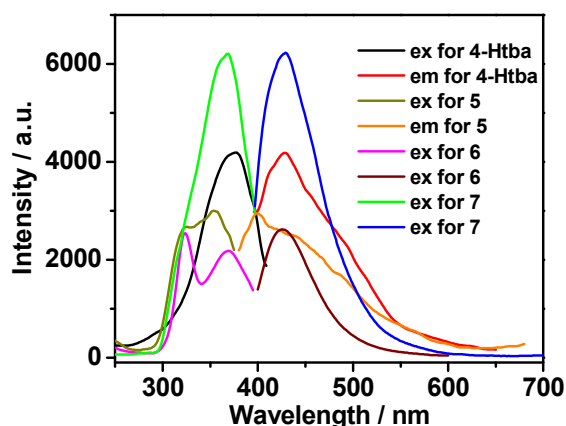

Fig. 11 The excitation and emission spectra of Cd(II) complexes **5–7** in solid state at room temperature (excitation slit: 5.0, emission slit: 2.5)

Table 3 Summary of solid-state photophysical data for **1**-**7**.

Compound	crystal density / g·cm-3	λex / nm	λmax / nm	blue shifts compared to 4-Htba / nm	Stokes shifts / nm
4-Htba	/	377	427	/	50
1	1.754	309	351	76	53
2	1.784	321	426	1	105
3	1.660	322	418	9	96
4	1.458	343	391	36	48
5	1.458	353	400	27	47
6	1.813	324	425	2	101
7	1.508	369	429	-2	60

fluorescent spectra of compounds **2**-**4** and **7** show significant enhancement in intensity, and **1** and **3**-**5** exhibit blue shifts of 76, 9, 36, and 27 nm, respectively. Their different emission behaviours may mainly originate from different metal centers, coordination modes of ligands, coordination angles of the ligands, the dihedral angles between benzene ring and triazole ring as well as weak interactions in the network lattice, which have close relationships to the photoluminescence behaviour. Furthermore, **1** displays very weak emission intensity in comparison to the organic ligand and other zinc complexes, which can be assigned to the occurrence of fluorescence quenching in **1**. The reason for fluorescence quenching may be due to the coordinated water molecules which may efficiently quench the fluorescence of compounds through high-energy O-H oscillators.[25] Besides, the crystal densities of dense structures **2** (1.784 g·cm^{-3}), **3** (1.660 g·cm^{-3}) and **6** (1.813 g·cm^{-3}) are also markedly higher than those of porosity structures **4** (1.458 g·cm^{-3}), **5** (1.458 g·cm^{-3}) and **7** (1.508 g·cm^{-3}), which imply the interligand contacts (Table S2†) and/or the network rigidities in the order of dense structure > porosity structure. Therefore, the lager Stokes shifts of dense structures **2** (105 nm), **3** (96 nm) and **6** (101 nm) may be ascribed to that the strong interligand contacts and/or the network rigidities change HOMO-LUMO gaps of intraligand transitions, which increasing the excited state distortion and nonradiative transitions.

Conclusions

In conclusion, a serial of Zn(II)/Cd(II) complexes have been synthesized under hydro/solvothermal conditions by using a triazolate-carboxylate bifunctional ligand, and their structures vary from discrete mononuclear structure, two-dimension (2D) non-interpenetrating layer, 2D 2-fold interpenetrating layer, 4-fold interpenetrating dia network, 5-fold interpenetrating dia framework to 3D, decanuclear cadmium-chloride chain-based porous framework. The diverse structures of the compounds are caused by different coordination modes of the central metal ions and the organic ligands as well as the different reaction conditions. In addition, the thermal stability and photoluminescence properties of these complexes have been

investigated, and reveal that the dense structures **2**, **3** and **6** display higher thermal stability and bluish-purple emissions with larger Stokes shifs, which may serve as candidates for luminescent materials.
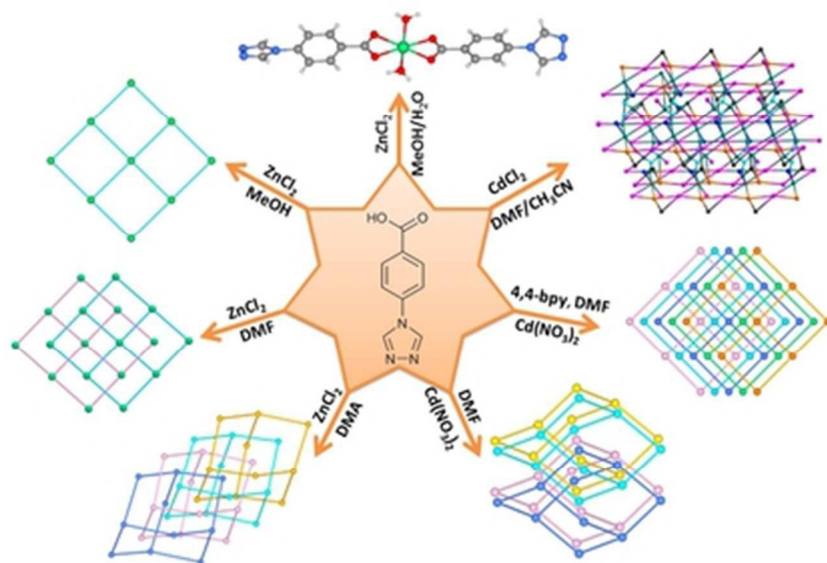
Acknowledgements

Notes and references

1   (a) M. Eddaoudi, D. B. Moler, H. Li, B. Chen, T. M. Reineke, M. O'Keeffe and O. M. Yaghi, *Acc. Chem. Res.*, 2001, **34**, 319; (b) M. O'Keeffe and O. M. Yaghi, *Chem. Rev.*, 2012, **112**, 675; (c) M. Li, D. Li, M.O'Keeffe and O. M. Yaghi, *Chem. Rev.*, 2014, **114**, 1343.

2   (a) M. P. Suh, H. J. Park, T. K.Prasad and D.-W. Lim, *Chem. Rev.*, 2012, **112**, 782; (b) K. Sumida, D. L. Rogow, J. A. Mason, T. M. McDonald, E. D. Bloch, Z. R. Herm, T.-H. Bae and J. R. Long, *Chem. Rev.*, 2012, **112**, 724; (c) R. B. Getman, Y.-S. Bae, C. E. Wilmer and R. Q. Snurr, *Chem. Rev.*, 2012, **112**, 703; (d) Y. He, W. Zhou, G. Qian and B. Chen, *Chem. Soc. Rev.*, 2014, **43**, 5657; (e) H. Wu, Q. Gong, D. H. Olson and Jing Li, *Chem. Rev.*, 2012, **112**, 836.

3   (a) J.-R. Li, R. J. Kuppler and H.-C. Zhou, *Chem. Soc. Rev.*, 2009, **38**, 1477; (b) J.-R. Li, J. Sculley and H.-C. Zhou, *Chem. Rev.*, 2012, **112**, 869; (c) B. V. Voorde, B. Bueken, J. Denayerb and D. D. Vos, *Chem. Soc. Rev.*, 2014, **43**, 5766.

4   (a) T. Maji, R. Matsuda and S. Kitagawa, *Nature*, 2007, **6**, 142.; (b) C. K. Brozek and M. Dincă, *Chem. Soc. Rev.*, 2014, **43**, 5456; (c) B. Manna, S. Singh, A. Karmakar, A. V. Desai and S. K. Ghosh, *Inorg. Chem.*, 2015, **54**, 110.

5   (a) L. Ma, C. Abney and W. Lin, *Chem. Soc. Rev.*, 2009, **38**, 1248; (b) A. Corma, H. García and F. X. L. Xamena, *Chem. Rev.*, 2010, **110**, 4606; (c) M. Yoon, R. Srirambalaji and K. Kim, *Chem. Rev.*, 2012, **112**, 1196; (d) A. Dhakshinamoorthy and H. Garcia, *Chem. Soc. Rev.*, 2014, **43**, 5750; (e) J. Liu, L. Chen, H. Cui, J. Zhang, L. Zhang and C.-Y. Su, *Chem. Soc. Rev.*, 2014, **43**, 6011.

6   (a) M. Kurmoo, *Chem. Soc. Rev.*, 2009, **38**, 1353; (b) P. Dechambenoit and J. R. Long, *Chem. Soc. Rev.*, 2011, **40**, 3249; (c) E. Coronado and G. M. Espallargas, *Chem. Soc. Rev.*, 2013, **42**, 1525;(d) W.-X. Zhang, P.-Q. Liao, R.-B. Lin, Y.-S. Wei, M.-H. Zeng and X.-M. Chen, *Coord. Chem. Rev.*, 2015, **293–294**, 263.

7   (a) L. E. Kreno, K. Leong, O. K. Farha, M. Allendorf, R. P. Van Duyne and J. T. Hupp, *Chem. Rev.*, 2012, **112**, 1105; (b) Y. Cui, Y. Yue, G. Qian and B. Chen, *Chem. Rev.*, 2012, **112**, 1126; (c) Z. Hu, B. J. Deibert and J. Li, *Chem. Soc. Rev.*, 2014, **43**, 5815.

8   (a) M. Du, C.-P. Li, C.-S. Liu and S.-M. Fang, *Coord. Chem. Rev.*, 2013, **257**, 1282; (b) F. A. A. Paz, J. Klinowski, S. M. F. Vilela, J. P. C. Tomé , J. A. S. Cavaleiro and J. Rocha, *Chem. Soc. Rev.*, 2012, **41**, 1088; (c) W. Lu, Z. Wei, Z.-Y. Gu, T.-F. Liu, J. Park, J. Park, J. Tian, M. Zhang, Q. Zhang, T. Gentle III, M. Bosch and H.-C. Zhou, *Chem. Soc. Rev.*, 2014, **43**, 5561.

9   (a) H.-L. Jiang, T. A. Makal and H.-C. Zhou, *Coord. Chem. Rev.*, 2013, **257**, 2232; (b) A. Santra and P. K. Bharadwaj, *Cryst. Growth Des.*, 2014, **14**, 1476; (c) N. Wei, M.-Y. Zhang, X.-N. Zhang, G.-M. Li, X.-D. Zhang and Z.-B. Han, *Cryst. Growth Des.*, 2014, **14**, 3002; (d) Z. Ju and D. Yuan, *CrystEngComm*, 2013, **15**, 9513; (e) Y.-F. Hou, B. Liu, K.-F. Yue, C.-S. Zhou, Y.-M. Wang, N. Yan and Y.-Y. Wang, *CrystEngComm*, 2014, **16**, 9560; (f) J. Duan, M. Higuchi, C. Zou, W. Jin and S. Kitagawa, *CrystEngComm*, 2015, **17**, 5609.

10 (a) B. Zheng, J. H. Luo, F. Wang, Y. Peng, G. H. Li, Q. S. Huo and Y. L. Liu, *Cryst. Growth Des.*, 2013, **13**, 1033; (b)J. Bai, H.-L. Zhou, P.-Q. Liao, W.-X. Zhang and X.-M. Chen, *CrystEngComm*, 2015, **17**, 4462; (c) Y.-F. Peng, S. Zhao, K. Li, L. Liu, B.-L. Li and B. Wu, *CrystEngComm*, 2015, **17**, 2544.

11 (a) Y. Yu, L. Zhang, Y. Zhou and Z. Zuhra, *Dalton Trans.*, 2015, **44**, 4601; (b) T.-W. Tseng, T.-T. Luo, C.-C. Su, H.-H. Hsu, C.-I Yang and K.-L. Lu, *CrystEngComm*, 2014, **16**, 2626; (c) S. Yuan, S.-S. Liu and D. Sun, *CrystEngComm*, 2014, **16**, 1927; (d) L. Wang, Z.-H. Yan, Z. Xiao, D. Guo, W. Wang and Y. Yang, *CrystEngComm*, 2013, **15**, 5552.

12 (a) H.-L. Jiang and Q. Xu, *CrystEngComm*, 2010, **12**, 3815; (b) Z. Su, Y. Zhao, M. Chen and W.-Y. Sun, *CrystEngComm*, 2011, **13**, 1539; (c) Z. Xue, T. Sheng, Y. Wen, Y. Wang, S. Hu, R. Fu and X. Wu, *CrystEngComm*, 2015, **17**, 598; (d) M. E. Carnes, N. R. Lindquist, L. N. Zakharov and D. W. Johnson, *Cryst. Growth Des.*, 2012, **12**, 1579.

13 (a) S. Kitagawa, R. Kitaura and S.-I. Noro, *Angew. Chem., Int. Ed.*, 2004, **43**, 2334; (b) F. A. A. Paz, J. Klinowski, S. M. F. Vilela, J. P. C. Tomé, J. A. S. Cavaleiro and J. Rocha, *Chem. Soc. Rev.*, 2012, **41**, 1088; (c) Y. He, B. Li, M. O'Keeffe and B. Chen, *Chem. Soc. Rev.*, 2014, **43**, 5618; (d) G. Aromí, L. A. Barrios, O. Roubeau and P. Gamez, *Coord. Chem. Rev.*, 2011, **255**, 485; (e) J.-P. Zhang, Y.-B. Zhang, J.-B. Lin and X.-M. Chen, *Chem. Rev.*, 2012, **112**, 1001.

14 (a) Z. Su, Y. Zhao, M. Chen and W.-Y. Sun, *CrystEngComm*, 2011, **13**, 1539; (b) C.-T. He, J.-Y. Tian, S.-Y. Liu, G. Ouyang, J.-P. Zhang and X.-M. Chen, *Chem. Sci.*, 2013, **4**, 351; (c) P. Pachfule, Y. Chen, S. C. Sahoo, J. Jiang and R. Banerjee, *Chem. Mater.*, 2011, **23**, 2908; (d) F. Nouar, J. F. Eubank, T. Bousquet, L. Wojtas, M. J. Zaworotko and M. Eddaoudi, *J. Am. Chem. Soc.*, 2008, **130**, 1833; (e) D.-X. Xue, A. J. Cairns, Y. Belmabkhout, L. Wojtas, Y. Liu, M. H. Alkordi and M. Eddaoudi, *J. Am. Chem. Soc.*, 2013, **135**, 7660; (f) Q. Zhang, H. Zhang, S. Zeng, D. Sun and C. Zhang, *Chem.-Asian J.*, 2013, **8**, 1985; (g) Q. Zhang, A. Geng, H. Zhang, F. Hu, Z.-H. Lu, D. Sun, X. Wei and C. Ma, *Chem.-Eur. J.*, 2014, **20**, 4885.

15 (a) M. Chen, S.-S. Chen, T.-A. Okamura, Z. Su, M.-S. Chen, Y. Zhao, W.-Y. Sun and N. Ueyama, *Cryst. Growth Des.*, 2011, **11**, 1901; (b) T. Panda, P. Pachfule and R. Banerjee, *Chem. Commun.*, 2011, **47**, 7674; (c) T. Panda, T. Kundu and R. Banerjee, *Chem. Commun.*, 2012, **48**, 5464; (d) J. Xiao, Y. Wu, M. Li, B.-Y. Liu, X.-C. Huang and Dan Li, *Chem.-Eur. J.*, 2013, **19**, 1891; (e) T. Li, J. Yang, X.-J. Hong, Y.-J. Ou, Z.-G. Gu and Y.-P. Cai, *CrystEngComm*, 2014, **16**, 3848; (f) Y.-L. Wang, J.-H. Fu, J.-J. Wei, X. Xu, X.-F. Li and Q.-Y. Liu, *Cryst. Growth Des.*, 2012, **12**, 4663; (g) M. Du, C.-P. Li, M. Chen, Z.-W. Ge, X. Wang, L. Wang and C.-S. Liu, *J. Am. Chem. Soc.*, 2014, **136**, 10906; (h) W.-Y. Gao, R. Cai, L. Meng, L.Wojtas, W. Zhou, T. Yildirim, X. Shi and S. Ma, *Chem. Commun.*, 2013, **49**, 10516; (i) S. I. Vasylevs'kyy, G. A. Senchyk, A. B. Lysenko, E. B. Rusanov, A. N. Chernega, J. Jezierska, H. Krautscheid, K. V. Domasevitch and A. Ozarowski, *Inorg. Chem.*, 2014, **53**, 3642; (j) A.-X. Zhu, Z.-Z. Qiu, L.-B. Yang, X.-D. Fang, S.-J. Chen, Q.-Q. Xu and Q.-X. Li, *CrystEngComm*, 2015, **17**, 4787.

16 (a) J.-F. Song, R.-S. Zhou, J. Zhang, C.-Y. Xu, Y.-B. Li and B.-B. Wang, *Z. Anorg. Allg. Chem.*, 2011, **637**, 589; (b) T. Aharen, F. Habib, I. Korobkov, T. J. Burchell, R. Guillet-Nicolas, F. Kleiz and M. Murugesu, *Dalton Trans.*, 2013, **42**, 7795; (c) R. J. Holmberg, M. Kay, I. Korobkov, E. Kadantsev, P. G. Boyd, T. Aharen, S. Desgreniers, T. K. Woo and M. Murugesu, *Chem. Commun.*, 2014, **50**, 5333; (d) D.-M. Chen, W. Shi and P. Cheng, *Chem. Commun.*, 2015, **51**, 370; (e) D.-M. Chen, J.-G. Ma and P. Cheng, *Dalton Trans.*, 2015, **44**, 8926.

17 G. M. Sheldrick, *SADABS, Program for Rigaku R-AXIS SPIDER diffractometer Absorption Correction,* University of Göttingen, Göttingen, Germany, 1996.

18 T. Higashi, *ABSCOR, Program for Bruker Area Detector Absorption Correction*, Rigaku Corporation, Tokyo, Japan, 1995.

19 G. M. Sheldrick, *SHELXS-97 and SHELXL-97, Program for solution of crystal structures*, University of Göottingen, Germany, 1997.

20 A. L. Spek, *Acta Crystallogr., Sect. C: Struct. Chem.*, 2015, **71**, 9.

21 (a) S. Xu, W. Shao, M. Yu and G. Gong, *Acta Crystallogr. Sect. E: Struct. Rep. Online*, 2011, **67**, m728; (b) L.V. Lukashuk, A. B. Lysenko, E. B. Rusanov, A. N. Chernega and K. V. Domasevitch, *Acta Crystallogr., Sect. C: Struct. Chem.*, 2007, **63**, m140.

22 The trigonallity index τ (τ = 0 denotes ideal square pyramidal; τ = 1 denotes ideal trigonal bipyramidal) was calculated according to the literature. See: A. W. Addison, T. N. Rao, J. Reedijk, J. van Rijn and G. C. Verschoor, *J. Chem. Soc., Dalton Trans.*, 1984, 1349.

23 (a) K.-H. Cui, S.-Y. Yao, H.-Q. Li, Y.-T. Li, H.-P. Zhao, C.-J. Jiang and Y.-Q. Tian, *CrystEngComm*, 2011, **13**, 3432; (b) S. N. Wang, R. R. Yun, Y. Q. Peng, Q. F. Zhang, J. Lu, J. M. Dou, J. F. Bai, D. C. Li and D. Q. Wang, *Cryst. Growth Des.*, 2012, **12**, 79; (c) S.-S. Chen, Q. Liu, Y. Zhao, R. Qiao, L.-Q. Sheng, Z.-D. Liu, S. Yang and C.-F. Song, *Cryst. Growth Des.*, 2014, **14**, 3727.

24 (a) H. He, F. Sun, H. Su, J. Jia, Q. Li and G. Zhu, *CrystEngComm*, 2014, **16**, 339; (b) Y. Yang, J. Yang, P. Du, Y.-Y. Liu and J.-F. Ma, *CrystEngComm*, 2014, **16**, 1136; (c) K. Liu, Y. Peng, F. Yang, D. Ma, G. Li, Z. Shi and S. Feng, *CrystEngComm*, 2014, **16**, 4382; (d) J. Li, T. Sheng, S. Bai, S. Hu, Y. Wen, R. Fu, Y. Huang, Z. Xue and X. Wu, *CrystEngComm*, 2014, **16**, 2188.

25 (a) D.-L. Yang, X. Zhang, Y.-G. Yao and J. Zhang, *CrystEngComm*, 2014, **16**, 8047; (b) B. Chen, Y. Yang, F. Zapata, G. Qian, Y. Luo, J. Zhang and E. B. Lobkovsky, *Inorg. Chem.*, 2006, **45**, 8882.

CrystEngComm

ARTICLE

Seven d^{10} coordination compounds based on a triazolate-carboxylate bifunctional ligand have been synthesized and structurally characterized. Their thermal stability and photoluminescence properties were also investigated.

37x24mm (300 x 300 DPI)